Performance Analysis of WECS with Hill-Climbing MPPT Technique and Improved FRT Method

Vangala Ravalika[1], Lalu Mudavath[2], Dr. T. Anil Kumar[3]

[1]PG-Scholar, Department of EEE, Anurag University, Hyderabad, India

[2]Assistant professor, Department of EEE, Anurag University, Hyderabad, India

[3]Head of Department, Department of EEE, Anurag University, Hyderabad, India

ravalikavangala@gmail.com[1],lalueee@cvsr.ac.in[2], hodeee@cvsr.ac.in[3]

Abstract:

Using a Hill-climbing maximum power point tracker and DFIG, to analyse the fault-tolerance of a wind power system. There have been a number of reports of by using the Hill-Climbing Strategy to improve the performance of their MPPT systems. Modalities such as incremental conductance and P & O are also appropriate here. In this paper, a fault-ride through (FRT) system for a wind turbine with a DFIG, which is resilient to symmetrical and unbalanced grid voltage sags due to the efficient use of Hill-climbing (HC) maximum power point tracking (MPPT) control. In a wind energy conversion system, this is accomplished via the rotor power converter system, which regulates the voltage across the stator. The voltage dropssignificantly boosted by the FRT's capacity, allowing the stator and rotor currents to be maintained at levels substantially below the minimum necessary for safe operation. Since the new topology requires no additional hardware and the old one can be quickly changed, the control system and its implementation are very cost-effective. The feasibility and practical benefits of the proposed HC-MPPT and FRT control technique are shown by simulations of both large and small scale WECS with DFIG.

Keywords: Wind energy conversion system, doubly-fed induction generator, hill-climbing maximum power point tracking, and fault ride through.

DOI Number: 10.48047/NQ.2022.20.20.NQ109104 **NeuroQuantology2022;20(20): 1053-1064**

1. INTRODUCTION

However, in order for wind power to become prevalent, it will be essential to construct turbines that can create energy and feed that electricity back into the grid through FRT. However, the speed with which things return to normal once a voltage drop has been rectified depends on the system's ability to sustain continuous energy output and manage current variations. But if a considerable proportion of wind power suddenly stopped functioning, it might cause significant problems for the network [2]. Since DFIGs' stator windings are hardwired to the grid and the rotor side conversion mechanism regulates only a tiny fraction of the power generated, they are very susceptible to grid disruptions. Since symmetric and asymmetric network failures are so common, WECS cannot continue to operate without the FRT capabilities of DFIGs. Because the magnetic flux does not react quickly enough to the abrupt change in stator voltage, a DFIG has overvoltage and overcurrent transients while the rotor is spinning. In the event of an asymmetrical breakdown, if the stator voltage has a negative sequence component and the slip frequency is large, overvoltage and overcurrent oscillations may arise. There have been several research conducted on the FRT problem in a WECS with DFIG, and the outcomes may be broken down into two groups: hardware interventions and control upgrades. Most FRT techniques, such as physically limiting the rotor winding connections with a crowbar, safeguard the rotor side power converters against voltage and current transients [5, 6]. The crowbar has to make contact with the rotor's driving winding to cause a short circuit. The DFIG might be mistaken for an induction generator with this configuration. The amount of voltage supports the DFIG can give is diminished by the reactive power it must spend to suppress large transient stator currents. The same action may be performed with significantly less force using voltage fluctuations across a dc connection, as illustrated in [8], as opposed to the "crowbar control" shown in [7]. The motor can be protected from overvoltage if the dc-capacitor voltage is high enough, and crowbars in the rotor winding can be timed to activate with the dc-link [9]. Professional technical writers have invested many hours in studying and practicing FRT techniques. Among the many applications for devices based on superconductors are those that restrict current in fault circuits [17-19] and those that dynamically restore voltage in a circuit [10-12]. To keep the output voltage stable, voltage compensators that are wired in series with the stator [13], rotor [14], and grid cycle on and off at regular intervals. A FRT system with series impedance and a rotor crowbar may be useful for saturated core fault current limiters, which normally must account for the same permeability difference between the saturated and unsaturated states. We examine the operation and small-signal performance of a WECS-DFIG that is coupled to a high-impedance, low-voltage ac grid.

It is shown that low-voltage FRT may benefit from transient reconfiguration control of the power converters in the WECS. This prototype hybrid FRT system tests a grid-side rectifier in parallel, a grid-side converter in series, a battery, and a switch-type fault current limiter. In [12], a rotor-side converter is combined with a grid-side converter to achieve FRT, and in [15], a four-switch design with a halfway connection is outlined in great detail to illustrate FRT in practice. Extensive study has been dedicated to enhancing the DFIG control capabilities of a WECS by enhancing its FRT capabilities. When power is unavailable, a PI controller with a vector hysteresis current regulator is your best bet. With the use of flux-linkage tracking, we can learn how to design a crowbar-free FRT control system for a brushless DFIG by analyzing a source with voltage dips of constant amplitude. Taking into account all of this information, it is reasonable to conclude that implementing the proposed FRT solutions that involve hardware modifications would be effective at achieving the FRT objectives, but would also require the acquisition of additional hardware, thereby increasing the cost of the WECS. Improved FRT control may increase capacity if the control system can't manage the load, but it will reduce dependability. Our results show that studying the FRT in a WECS with DFIG requires additional investigation. The WECS-DFIG is responsible for reliably addressing both symmetric and asymmetric voltage drops, so it must be cost-effective, user-friendly, and dependable. Grid voltage drops can be detected using tools like phase locked loops, synchronous rotating reference frames, and symmetrical component algorithms. Applying a voltage harmonic footprint and matrix strategy can lessen phase shift and grid voltage loss. The official WECS with DFIG documentation explains the various voltage detection strategies in detail. Hilbert-Huang transforms, nonlinear adaptive filters, and extended second-order integrators are a few examples of such methods. This project's overarching goal is to develop a fault-tolerant, deployable, and controllable WECS-DFIG that won't drive up deployment costs or control system complexity. In the event of an electrical grid breakdown, the proposed system's fault-ride-through capabilities reduce the production of potentially dangerous transient current and voltage.Both symmetric and asymmetric voltage reductions have no negative effect on the suggested FRT configuration's performance. Adjusting the stator voltage when running the WECS in DFIG mode is necessary to keep the nominal value constant regardless of the grid voltage. It's not required to use problem-solving techniques because of this. For the reason why a grid-side converter may regulate the stator voltage in a rotor power conversion system. Enhanced DFIG administration of a WECS was a driving factor in the development of this controller. After modifying the network's foundation in suitable ways, we were able to include FRT and DFIG into a WECS. By controlling the stator voltage directly, the proposed technique mitigates grid power interruptions induced by FRT systems, which are addressed in the technical literature. This topology may be built with little time or money spent on it since it requires only minor adjustments to the typical WECS structure. For maximum efficiency, the central generator in a wind power system must have a power factor of 1, as required by the FRT principle. The WECS-settings allow DFIG to operate on a wide variety of power factors. Grid imbalances and symmetric and asymmetric voltage drops are taken into account in the simulation's findings. What follows is a brief abstract of the paper's main arguments and conclusions.

2. PROPOSED SYSTEM

Topology of Fault Tolerant Wecs with DFIG

Fig. 1 depicts a typical use of DFIG in WECS (wireless eavesdropping and communication systems). (a). A generator side converter (GeSC) produces electricity at the rotor and is then delivered via a grid side converter (GSC). To power the FRT, which is propelled by a crowbar resistance, the battery regulates voltage and current (BSS). As can be observed in Fig. 1, a common rotor-side converter pair consists of a generator (Gas) and a grid (Gs') device. (a). The lack of Dangerous Behavior Enhanced techniques of energy storage and a crowbar-shaped device for deflecting force are presented (FRT) (FRT) As can be observed in Figure 1(a), grid voltage variations affect the stator voltage of DFIG, and hence the efficiency of the WECS. If the FRT's stator voltage can be adjusted, it would be feasible to reduce the power grid's voltage drop. The problem was solved by decreasing the voltage and current output. One possible approach to doing this is the WECS-DFIG configuration seen in Fig. 1. Connecting the secondary windings ofgrid transformer to the DFIG stator generates a series connection. The primary windings of transformer are connected to the power grid through this wire. Depending on the actual grid voltage, the Grosch may be able to keep the DFIG's stator voltage at its nominal value. Since WECSs with DFIGs are protected from transient currents caused by grid disturbances, they may continue operating normally even when these currents are present (see Figure 6.1, which displays a multi-wound grid transformer). In contrast, the suggested FRT architecture requires just two single-wound transformers. However, when the rotor and stator of a motor share a single coil, the rotor will provide just half of the stator's output. In Figure 1, we can see how the secondary rotor winding of DFIG's transformer is connected to the main generating winding of grid transformer. Some of the advantages of using a DFIG are that it can control the voltage on the rotor and isolate the stator from the rotor. By keeping the Grosch in the configuration depicted in Figure 6.1b, you may avoid the necessity for a crowbar-proof control system. By doing so, the system's dependability and capacity to tolerate errors will improve. The low-pass (LCL) filter in the FRT architecture is driven by the inductances of the rotor transformer rather than resonant capacitors. The crowbar might be powered by two inexpensive single-winding transformers rather of the complex multi-winding transformer seen in Fig.1. After FRT is put into place, we do not expect any adjustments to the WECS tariffs.

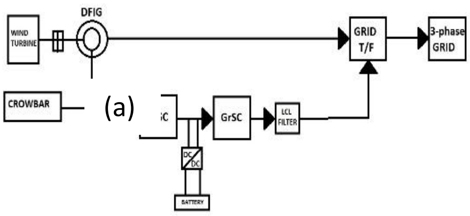

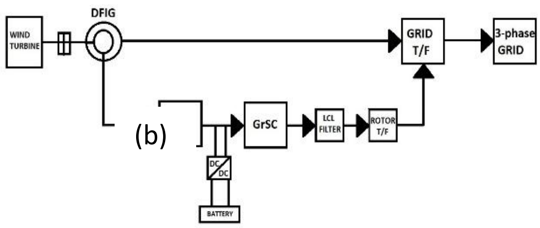

Fig. 1: An analysis of the DFIG and WECS in their (a)original (b) and improved (with FRT) forms.

Any effective power management system will need a dc-dc converter and battery bank (BSS). For the FRT control to function as expected, the BSS in the WECS design must keep the dc-link voltage stable (Fig. 1(b)), as shown. This fits with the fact that the cost of the WECS as a whole is heavily dependent on the creation of electricity and the expansion of the related power infrastructure. To save expenses, WECS DFIGs have modified their standard FRT setup. When compared to traditional systems, the WECS is just as cost-effective because to the topological alterations included for fault tolerance (Fig. 1). For this reason, it is currently challenging to develop credible predictions of how much the wind system will cost, as it has its own unique technological requirements and the price of the necessary equipment is always fluctuating. Although the grid transformer in Fig.1(a) has low power losses and high system efficiency, the recommended FRT design in Fig.1(b) does not fare as well due to the additional iron loss in the core of rotor transformer. Since the rotor transformer operates at a lower voltage than the grid transformer, its additional iron loss (Figure1(b)) is less severe. The LCL filter in Fig.2 outperforms the standard WECS in Fig.1 thanks to its lower iron and copper losses, higher working voltage, and additional windings.Data demonstrates little to no performance loss for the suggested FRT structure when a DFIG is utilized to build a WECS.

FRT Control in Wecs With DFIG

When the stator flux-linkage inDFIG is perpendicular to the d-axis, decoupling control is available.

$$\psi_{qs} = 0 \quad (1)$$

Considering that

$$\psi_{qs} = L_{ls} I_{qs} + L_m (I_{qs} + I_{qr}) \quad (2)$$

Results

$$I_{qr} = -\frac{L_m + L_{ls}}{L_m} I_{qs} \quad (3)$$

The rotor's magnetizing and leakage inductances are represented by Lom and LLCs, while the stator's q- and d-axis flux linkages are shown by square and ds. The reactive power of a DFIG's stator may be determined with the use of the following formula.

$$Q_s = 1.5(I_{ds} V_{qs} - I_{qs} V_{ds}) \quad (4)$$

Were

$$V_{qs} = R_s I_{qs} + \omega_e \psi_{ds} \quad (5)$$

$$V_{ds} = R_s I_{ds} + \omega_e \psi_{qs} \quad (6)$$

are the DFIG stator voltage's q and d axes, respectively. As a result of (1), we can

$$Q_s = 1.5 I_{ds} \psi_{ds} \omega_e \quad (7)$$

As can be seen in Fig. 1, the geometric center of the series connection betweenDFIG stator and the secondary windings ofrotor transformer is located near the primary windings of the grid transformer. Because the stator discharges reactive power (Q s=0) point of common connection to the grid, DFIGs have a power factor of 1. Reactive power for the rotor side of the DFIG can only be supplied by gas and not by any other fuels. The reactive powersupplied to both the grid transformers and the DFIG rotor. Since ds is obviously not equal to 0, it follows that

$$I_{ds} = 0 \quad (8)$$

By using (1) and (8) in (6),

$$V_{ds} = 0 \quad (9) \qquad \psi_{ds} = L_{ls} I_{ds} + L_m (I_{ds} + I_{dr}) \quad (10)$$

and due to (8),

$$\psi_{ds} = L_m I_{dr} \quad (11)$$

To calculate the d-axis current component in a DFIG rotor, one uses the formula

$$I_{dr} = \frac{V_{qs} - R_s I_{qs}}{\omega_e L_m} \quad (12)$$

air-gap flux-linkage thus

$$\psi_m = L_m I_{dr} \quad (13)$$

Considering that the PF atpoint of shared grid connection is 1, we might potentially employ The output of the Grass VoVo may be roughly estimated in this way.

$$V_{qCov} = n_R \left(V_{qs} - n_G V_{Gq} - I_{qs} R_{Tr} \right) \quad (14)$$

$$V_{dCov} = \omega_e L_{Tr} I_{qs} \quad (15)$$

The inductance of the rotor transformer and the low-pass filter must be determined.

Since the DFIG keeps the stator voltage at its nominal value, the rotor and stator currents are kept within their safe operating limits, allowing for continuous operation even when the grid voltage drops. Consequently, Vs. must be maintained at the nominal voltage of the stator. Consider the Grass's maximum output voltage, for example.

$$V_{qCov} = n_R \left(V_{s\_nom} - n_G V_{Gq} - I_{qs} R_{Tr} \right) \quad (16)$$

We need to calculate the rotor transformer and low-pass filter inductances.

When the grid voltage drops, the DFIG maintains nominal stator voltage, which allows the generator to continue operating by keeping the rotor and stator currents within safe limits. This means that the stator's rated voltage must be maintained at all times for Vs. As an example, consider the Grass's maximum voltage output.

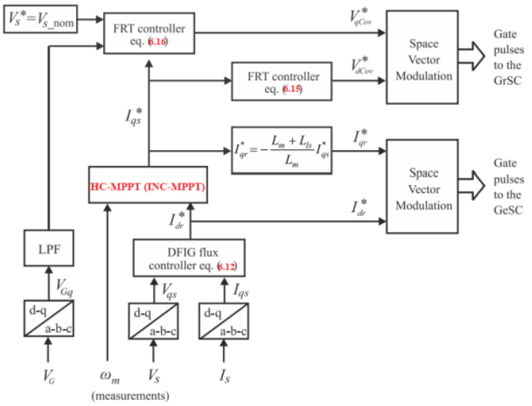

Fig. 2: New FRT control strategy for a WECS with DFIG.

2. HILL CLIMBING MPPT

Using HCS eliminates the need for a power meter, making the MPPT method more accessible. The concept was prompted by empirical evidence linking the rotational velocity of a turbine's shaft to its mechanical output. For HCS systems, the step size may be fixed or variable, or there might be two different yet complementary step sizes.

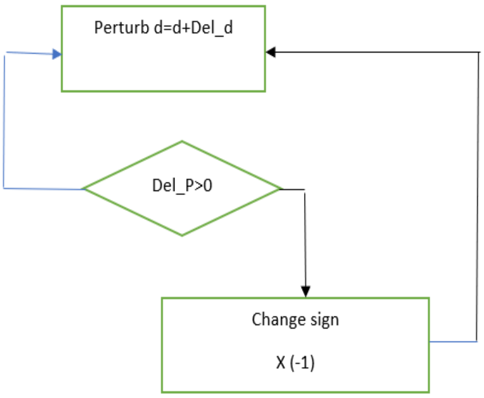

Fig. 3: Principle of HCS.

3. SIMULATION RESULTS

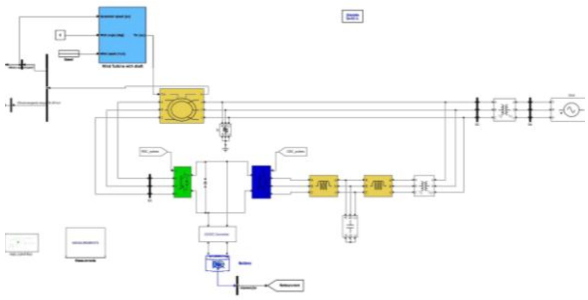

Fig. 4: MATLAB/SIMULINK circuit diagram of the system.

A) CURRENT CONTROL BASED MPPT WITH FRT[19]

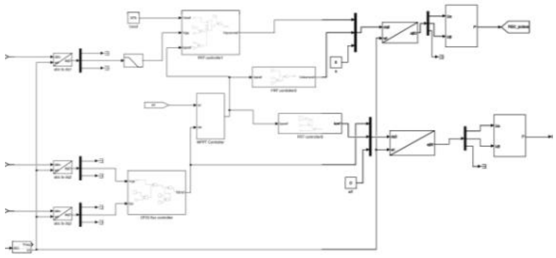

Fig. 5: Reference FRT control for WECS with DFIG.

Using a grid voltage disturbance that fluctuates symmetrically between 100% and 20% of the nominal value, the WECS is shown to work in both Fig. 5 (low wind speeds) and Fig. 6 (high wind speeds). Total harmonic distortion in the stator voltage drops by the same amount (20%) when the grid voltage drops (THD).

CASE-1:

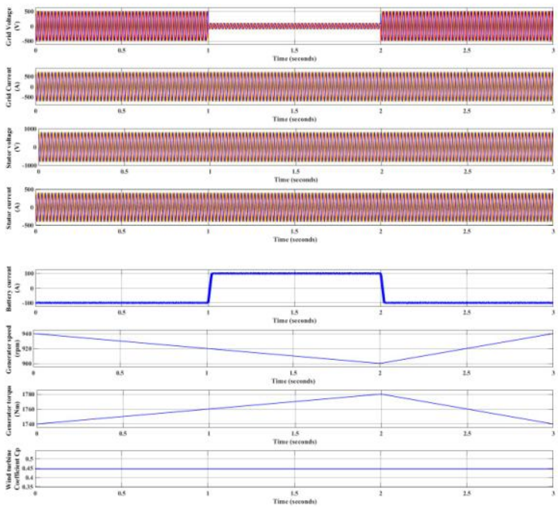

Fig. 6: Using a DFIG of 1.6 MW and a light wind speed = 4.5 m/s, the proposed FRT wind system was tested in a grid voltage disturbance that fluctuates symmetrically between 100% and 20% of the nominal voltage.

CASE-2:

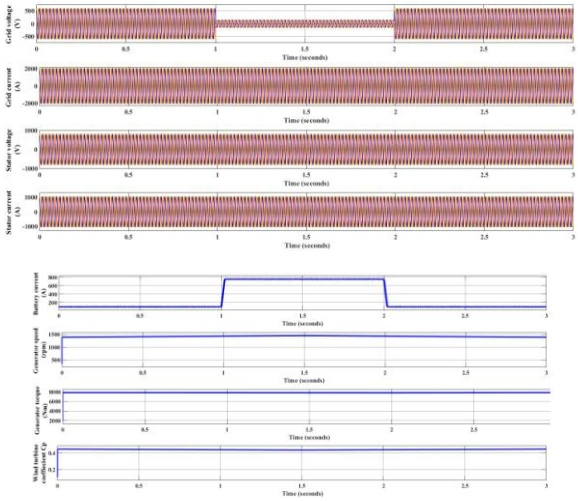

Fig. 7: The results of the simulations show that the FRT wind system with a DFIG of 1.6 MW can operate reliably in winds of up to 9 m/s and through grid voltage disturbance that fluctuates symmetrically between 100% and 20% of the nominal value.

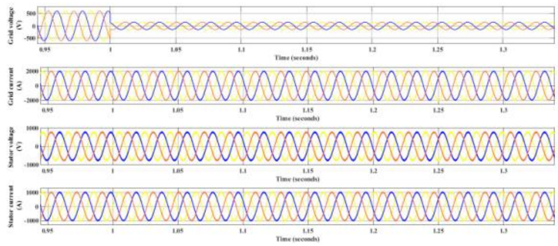

Fig. 8: Wind speed and grid voltage fluctuates (from 100% to 20% of nominal voltage) are accounted for in the simulation results (using WECS and a 1.6 MW DFIG) (in meters per second).

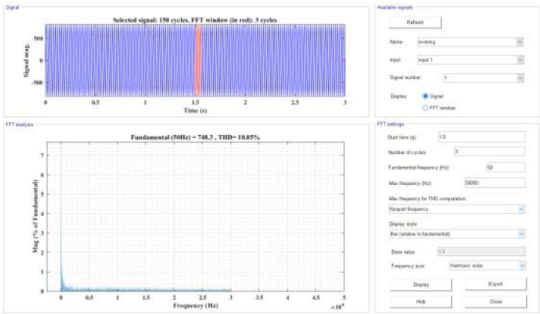

Fig. 9: THD% of stator voltage is 10.85%.

B) HILL CLIMBING MPPT TECHNIQUE WITH IMPROVED FRT

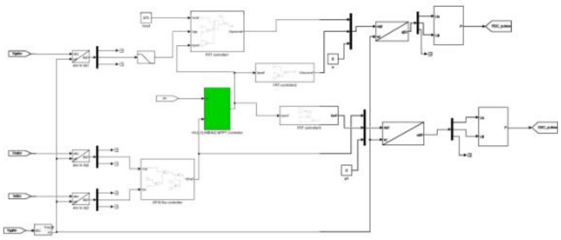

Fig. 10: Hill-climbing MPPT technique with improved FRT control for WECS with DFIG.

The output of the WECS is shown in images 11 (low wind speeds) and 12 (average wind speeds) grid voltage disturbance that fluctuates symmetrically between 100% and 20% of the nominal value. In

Fig. 13 and Fig. 14 the output of the WECS grid voltage disturbance that fluctuates symmetrically between 100%,20%,80% and back to the nominal value. Fig. 15 shows the reduction in harmonic distortion in stator voltage relative to the current setup.

CASE-1

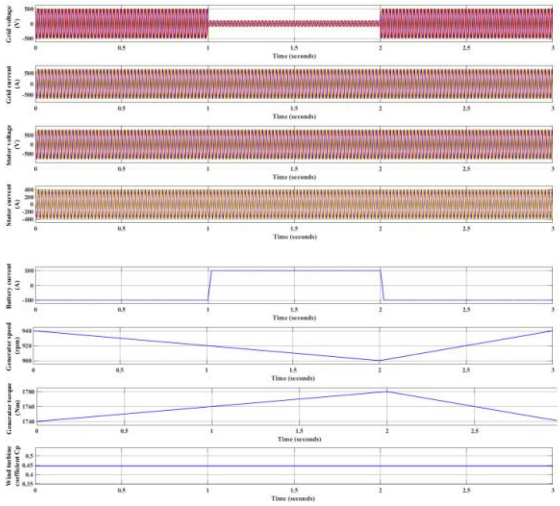

Fig. 11: Under low wind circumstances (4.5 m/s) grid voltage disturbance that fluctuates symmetrically between 100% and 20% of the nominal value,the DFIG of the anticipated FRT wind system was calculated to be 1.6 MW.

CASE-2

Fig. 12: The planned FRT wind system underwent wind tunnel testing at a constant speed = 9 m/s and a DFIG of 1.6 MW, with the system being subjected to 100%, 20%, and 100% grid voltage disturbances.

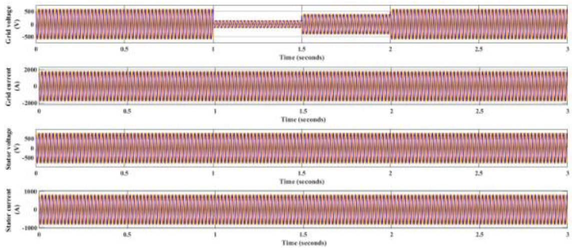

CASE-3

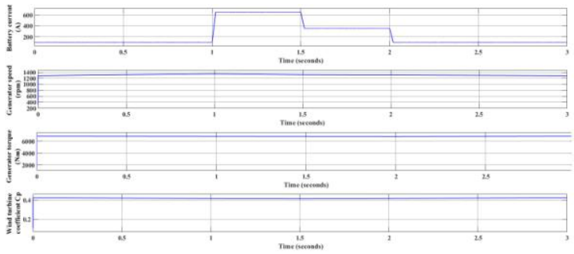

Fig. 13: Wind speed = 7m/s, grid voltage disturbance that fluctuates symmetrically 100%, 20%,80% back to 100% of the nominal value.

CASE-4

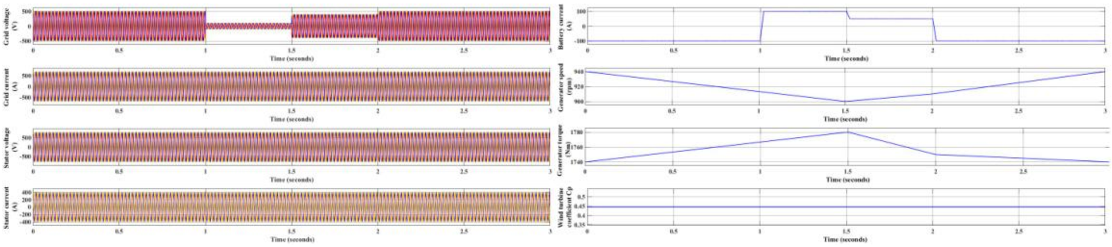

Fig. 14: Under low wind circumstances (4.5 m/s), grid voltage disturbance that fluctuates symmetrically 100%, 20%,80% back to100% of the nominal value.

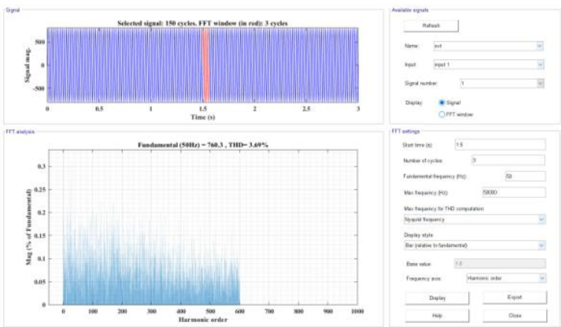

Fig. 15: THD% of stator voltage is 3.69%.

COMPARISION TABLE

	CURRENT CONTROL BASED MPPT WITH FRT	HILL CLIMBING MPPT TECHNIQUE WITH IMPROVED FRT
Stator Voltage THD%	10.85%	3.69%

4. CONCLUSION

In this paper, a DFIG-based WECS with hill climbing MPPT technique and improved FRT has been developed. The updated WECS system may be used to monitor and regulate the DFIG stator. It is possible, without a fault detection system, to keep the DFIG's stator voltage at its nominal value by fine-tuning the rotor-side converter. Therefore, the WECS consistently operates well regardless of whether the grid voltage is symmetrical, asymmetrical, or balanced. If the change is based on the exact substitution of expensive components of the traditional system with low-cost components and vice versa, then adopting the FRT control system proposed by WECS would increase overall cost as compared to the traditional system. Simulation have been done using 1.6 MW WECS-DFIG show that the suggested HC-MPPT-based FRT control method works and performs well. The proposed procedure reduces total harmonic distortion (THD).

REFERENCES

[1] E. Hau, Wind Turbines: Fundamentals, Technologies, Application, Economics, Springer-Verlag: 2013, 3rd Edition.

[2] A. El-Naggar and I. Erlich, 'Fault current contribution analysis of doubly fed induction generator-based wind turbines', IEEE Trans. Energy Conv., vol. 30, no. 3, pp. 874-882, Sept. 2015.

[3] D. Xiang, L. Ran, P.J. Tanner, and S. Yang, 'Control of a doubly fed induction generator in a wind turbine during grid fault ride-through', IEEE Trans. Energy Conv., vol. 21, no. 3, pp. 652-662, Sep. 2006.

[4] S. Seman, J. Niiranen, and A. Arkie, 'Ride-through analysis of doubly fed induction wind-power generator under unsymmetrical network disturbance', IEEE Trans. Power Syst., vol. 21, no. 4, pp. 1782–1789, Nov. 2006.

[5] J. Morren and S.W.H. de Haan, 'Ride through of wind turbines with doubly-fed induction generator during a voltage dip', IEEE Trans. Energy Conv., vol. 20, no. 2, pp. 435-441, June 2005.

[6] L.G. Megajoule, T. Littler, and D. Flynn, 'Decoupled-DFIG fault ride-through strategy for enhanced stability performance during grid faults', IEEE Trans. Sustain. Energy, vol. 1, no. 3, pp. 152-162, Oct. 2010.

[7] F.K.A. Lime, A. Luna, P. Rodriguez, E.H. Watanabe, and F. Blaabjerg, 'Rotor voltage dynamics in the doubly fed induction generator during grid faults', IEEE Trans. Power Electron., vol. 25, no. 1, pp. 118-130, Jan. 2010.

[8] L. Huchel, M.S. El Morsi, and H.H. Seinfeldian, 'A parallel capacitor control strategy for enhanced FRT capability of DFIG', IEEE Trans. Sustain. Energy, vol. 6, no. 2, pp. 303-312, April 2015.

[9] A.M.A. Haidar, K.M. Muttaqi, and M. Tarafdar, 'A coordinated control approach for DC link Nd roto crowbars to improve fault ride-through of DFIG-based wind turbine', IEEE Trans. Ind. Appl., vol. 53, no. 4, pp. 4073-4086, July/Aug. 2017.

[10] C. Wessels, F. Gebhardt, F.W. Fuchs, 'Fault ride-through of a DFIG wind turbine using a dynamic voltage restorer during symmetrical and asymmetrical grid faults', IEEE Trans. Power Electron., vol. 26, no. 3, pp. 807-814, March 2011.

[11] A.O. Ibrahim, T.H. Nguyen, D.C. Lee, and S.C. Kim, 'A fault ride through technique of DFIG wind turbine systems using dynamic voltage restorers', IEEE Trans. Energy Conv., vol. 26, no. 3, pp. 871-881, Sept. 2011.

[12] R.A. Amador payara, P. Kalian nan, S. Padmanaban, U. Subramaniam, and V.K. Ramachandra Murthy, 'Improved fault ride through capability in DFIG based wind turbines using dynamic voltage restorer with combined feed-forward and feed-back control', IEEE Access, vol. 5, no. 20494-20503, Oct. 2017.

[13] S. Zhang, K.J. Tseng, S.S. Choi, T.D. Nguyen, and D.L. Yao, 'Advanced control of series voltage compensation to enhance wind turbine ride through', IEEE Trans. Power Electron., vol. 27, no. 2, pp. 763-772, Feb. 2012.

[14] J. Mohammadi, S. Afshar Nia, S. Vaez-Zadeh, and S. Firangi, 'Improved fault ride through strategy for doubly fed induction generator-based wind turbines under both symmetrical and asymmetrical grid faults', IET Renew. Power Gener., vol. 10, no. 8, pp. 1114-1122, June 2016.

[15] P.H. Huang, M.S. El Morsi, S.A. Hasen, 'Novel fault ride-through scheme and control strategy for doubly fed induction generator-based wind turbine', IEEE Trans. Energy Conv., vol. 30, no. 2, pp. 635-645, June 2015.

[16] P.H. Huang, M. Shawky, W. Xiao, and J.L. Kirtley Jr., 'Novel fault ride through configuration and transient management scheme for doubly fed induction generator', IEEE Trans. Energy Conv., vol. 28, no. 1, pp. 86- 94, March 2013.

[17] M. Elsheikh, D.E.A. Mansour, and A.M. Azmy, 'Improving fault ride through capability of DFIG-based wind turbine using superconducting fault current limiter', IEEE Trans. Applied Superconductivity, vol. 23, no. 3, June 2013.

[18] L. Chen, C. Deng, F. Zheng, S. Yi, Y. Liu, and Y. Liao, 'Fault ride through capability enhancement of DFIG-based wind turbine with a flux-coupling-type SFCL employed at different locations', IEEE Trans. Appl. Superconductivity, vol. 25, no. 3, pp. 5201505, June 2015.

[19] Nikolaos Jabbour, EvangelosTsioumas, Christos Mademlis and EvgenySolomin, 'A Highly Effective Fault-Ride -Through Strategy for a Wind Energy C Conversion System with Doubly Fed Induction Generator', IEEE Trans. Power Electron., vol.35,no.8,pp.8154-8164,August 2020

eISSN 1303-5150